*Advances in Science and Technology*
*ISSN: 1662-0356, Vol. 102, pp 51-56*
*doi:10.4028/www.scientific.net/AST.102.51*

*Submitted: 2016-05-17*
*Accepted: 2016-06-27*
*Online: 2016-10-31*

# A Protease-Activated Ratiometric Fluorescent Probe for pH-Mapping of Malignant Tumor

Yi Hou[1, a *], Jin Zhou[1,b], Zhenyu Gao[2,c], Xiaoyu Sun[1,d], Chunyan Liu[1,e], Dihua Shangguan[1,f], Wensheng Yang[2,g] and Mingyuan Gao[1,h]

[1]Institute of Chemistry, the Chinese Academy of Sciences, Bei Yi Jie 2, Zhong Guan Cun, Beijing 100190, China,
[2]College of Chemistry, Jilin University, Changchun 130012, China.

[a]houyi@iccas.ac.cn, [b]zhoujin09@iccas.ac.cn, [c]gaozy10@mails.jlu.edu.cn, [d]sunxy@iccas.ac.cn, [e]liuchy@iccas.ac.cn, [f]sgdh@iccas.ac.cn, [g]wsyang@jlu.edu.cn, [h]gaomy@iccas.ac.cn

**Keywords:** $Fe_3O_4$ nanocrystals, protease-activated, pH mapping, ratiometric fluorescence, smart probe.

**Abstract.** A protease-activated ratiometric fluorescent probe based on fluorescence resonance energy transfer between a pH-sensitive fluorescent dye and biocompatible $Fe_3O_4$ nanocrystals was constructed. A peptide substrate of MMP-9 served as a linker between the particle quencher and the chromophore that was covalently attached to the antitumor antibody. The optical response of the probe to activated MMP-9 and gastric cell line SGC7901 tumor cells was investigated, followed by in vivo tumor imaging. Based on the ratiometric pH response to the tumor microenvironment, the resulting probe was successfully used to image the pH of subcutaneous tumor xenografts.

## Introduction

Tumor imaging remains a major player in the bioimaging field. In comparison with visualizing small malignant tumors, noninvasively extracting microenvironment information associated with tumor invasion and metastasis is more challenging. It is known that tumor microenvironment is strongly correlated with the growth, invasion, and metastasis of malignant tumors[1-9]. Therefore, developing noninvasive methods for detecting tumor microenvironment is very meaningful not only for tumor diagnosis, but also for predicting the risk of metastasis, the effectiveness of therapy, prognosis, etc. In long run, it will remarkably benefit the personalized medicine.

In principle, tumor cells need to breach extracellular matrixes to invade. Numerous studies have proven that matrix metalloproteases (MMPs), a family of zinc-dependent secreted endopeptidases, are involved in this process by regulating and processing the degradation of extracellular matrixes[2]. In addition, their over-expression correlates with advanced tumor stage, increased invasion and metastasis, and shortened survival[4-7]. Normally MMPs occur in unactivated form of zymogen, whereas they are activated and upregulated in almost all types of human cancers.

Apart from abnormal expression of proteases, tumor microenvironment is also characterized by abnormal extracellular pH, typically in a range of 6.2-6.9 slightly lower than that (7.2-7.4) for normal tissues as a result of anaerobic glycolysis[3]. The acidic environment of malignant tumors however leads to a significant number of harmful consequences, such as increased invasion and mutation rates, and radio resistance[8,9]. Thereby, monitoring the MMPs activity and pH in tumor region are very meaningful for cancer studies.

Optical detection has been demonstrated to be a facile and hypersensitive tool for biosensing, yet it suffers from the interference of autofluorescence of tissue regarding *in vivo* imaging[10]. One solution to reduce the background noise arising from the autofluroescence is to effectively quench the fluorescence of optical probes before they recognize the targets, and if the fluorescence can then be activated by endogenous enzymes, hypersensitive and enzyme-specific fluorescence probes can be realized[11-15].

Because of the unique physical properties, inorganic nanoparticles such as Au particles are largely chosen as a quencher for constructing hypersensitive optical probes based on fluorescence resonance energy transfer (FRET)[15]. In comparison with Au particles, iron oxide nanocrystals exhibit a broad featureless absorption covering large visible region due to the electronic transition of d-orbitals[16,17]. Therefore, magnetic iron oxide nanoparticles can principally be used a quencher for constructing FRET-based target-activatable optical probes, which remains to be explored yet. An additional benefit of using magnetic iron oxide particles instead of Au particles is that they can largely enhance the local contrast of magnetic resonance imaging, especially for tumors[18].

Regarding pH sensing, most fluorescent probes developed so far solely rely on the variation of fluorescence intensity, which is usually compromised by many non-pH factors such as the concentration of local chromophore. In contrast, ratiometric fluorescence probes can avoid such problem and thus allow quantitative determination of pH[19]. Herein, we develop a protease-activatable fluorescence imaging probe, and demonstrate the feasibility of this new probe design both *in vitro* and *in vivo*. In addition, imaging the pH of the tumor microenvironment was also achieved with calibration of the optical emissions.

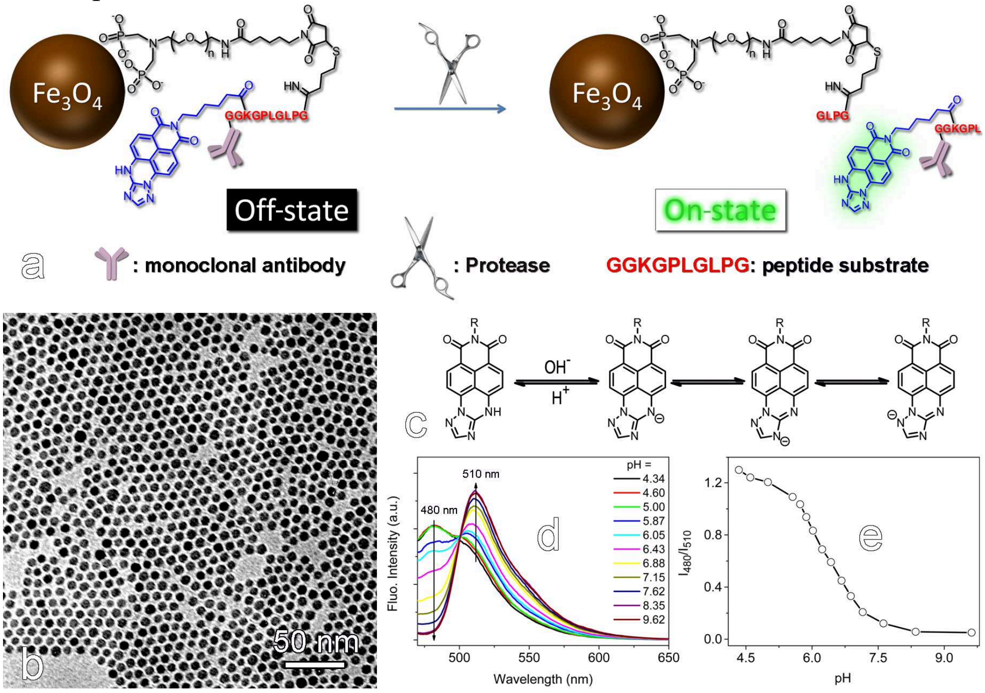


**Figure 1 | Construction of protease-activatable fluorescence imaging probe.** Schematic drawing of the protease-activatable fluorescence probe and its transition from "off-state" to "on-state" triggered by MMP-9 (a), TEM image of the as-prepared $Fe_3O_4$ nanoparticles (b),protonation/deprotonation induced structural transformation of ANNA (c), pH-depend fluorescence of ANNA recorded under excitation of 455 nm (d), and ratiometric fluorescence behavior of ANNA against pH (e).

**Construction of protease-activatable fluorescence imaging probe.** The protease-activatable fluorescence imaging probe was proposed based on $Fe_3O_4$ nanocrystal and ratiometric fluorescent dye that are covalently linked through a peptide substrate of MMP-9, as depicted in Fig. 1a. In its off-state, $Fe_3O_4$ particle is supposed to quench the fluorescence of the fluorescent dye, i.e., *N*-carboxyhexyl derivative of 3-amino-1,2,4-triazole fused 1,8-naphthalimide (ANNA), while in on-state the dye fluoresces after leaving the particle quencher upon detachment of the peptide linker via MMP-9. It is deserved to mention that a tumor-specific antibody covalently coupled to the C-terminal of the peptide substrate remains attached to the chromophores after the detachement, which helps to hold the chromophores in tumor extracellular matrix for the following pH-mapping. This design makes the current probe significantly different from those activatable probes reported before[11-15].

The $Fe_3O_4$ nanocrystals with an average size of 7.2 ± 0.6 nm, as shown in Fig. 1b, were prepared through a conventional thermal decomposition method by using oleic acid as surface ligands. By using an asymmetric polyethylene glycol (PEG) ligand bearing a diphosphate group at one end and a maleimide group at the other end to displace the hydrophobic ligands, PEGylated $Fe_3O_4$ nanoparticles were obtained. Via the maleimide group, ANNA-labeled peptide, i.e., Gly-Pro-Leu-Gly-Leu-Pro-Gly-Lys-Gly-Gly, was covalently linked to the particle surface, thereafter a gastric cancer specific antigastric cancer antibody $MGb_2$ was attached to the C-terminal of the peptide substrate through amidation reaction.

Due to the deprotonation and internal charge transfer from the electron-rich amino group to the electron-poor imide moiety, as illustrated in Fig. 1c, ANNA presents a strong pH dependent ratiometric emission as shown in Fig. 1d. The resulting intensity ratio of the fluorescence acquired at 480 nm and 510 nm, i.e., $I_{480}/I_{510}$, exhibits a sharp decrease especially in the range of 5.7-7.1 (Fig. 1e), which is especially interesting for detecting tumor-associated microenvironmental pH.

**Protease-response of nanoprobe.** The temporal protease-responsive behavior of the nanoprobe was evaluated in 1×PBS buffer (pH = 7.4) containing 15 nM activated MMP-9. As shown in Fig. 2a, the initial fluorescence intensity of the conjugate is rather weak, but is readily enhanced in the presence of MMP-9 by a factor of > 6 within 120 min as illustrated in Fig. 2b. In contrast, the fluorescence intensity of the probe remained nearly unchanged over 8 h in the absence of MMP-9 (off-state), which surely leads to excellent sensitivity in detecting MMP-9.

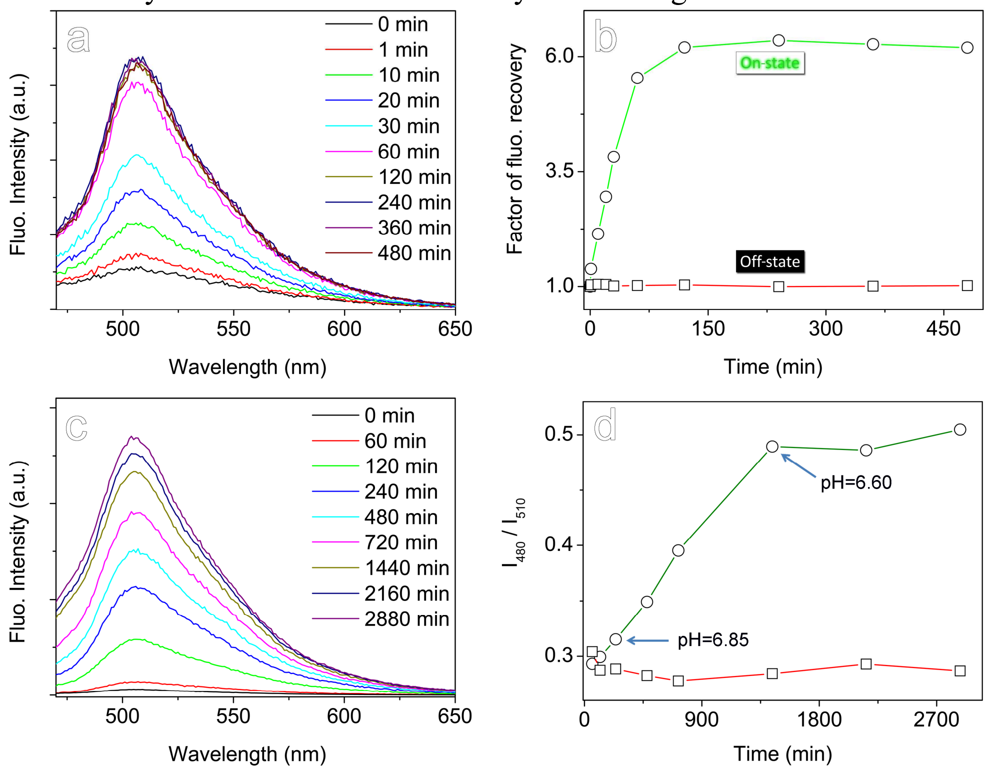


**Figure 2 | Protease-response of nanoprobe.** Fluorescence spectra of the probe incubated with the MMP-9 in 1×PBS buffer (a), temporal evolution of fluorescence peak intensity in the presence (green) or absence (red) of MMP-9 (b), fluorescence spectra of the probe incubated with SGC7901 cells (c), and ratiometric fluorescence behaviors recorded in the presence of SGC7901 cells (green), and human fibroblast cells (red) (d).

The cancer cell-responsive behavior of the probe was studied by incubating the final probe with tumor cells over-expressing MMP-9, i.e., human gastric cancer cell line SGC7901. The results shown in Fig. 2c clearly reveal that the fluorescence can effectively be activated by SGF7901 cells. According to the temporal evolution of $I_{480}/I_{510}$ ratio provided in Fig. 2d, the local pH for the chromophore remains above 6.85 during the early stage of incubation (<6 h), then it is decreased to approximately 6.60 while the $I_{480}/I_{510}$ ratio enters into a plateau region after 24 h incubation. The lowered pH is probably associated with the lysosomal process following the endocytosis of the fluorescent moiety remaining attached to the antibody. Nevertheless, roughly 90% of the chromophores remain located on the cell membrane if assuming the local pH of lysosome is around 5.0, which is greatly in favor of the detection of extracellular pH of tumors in the following *in vivo* studies.

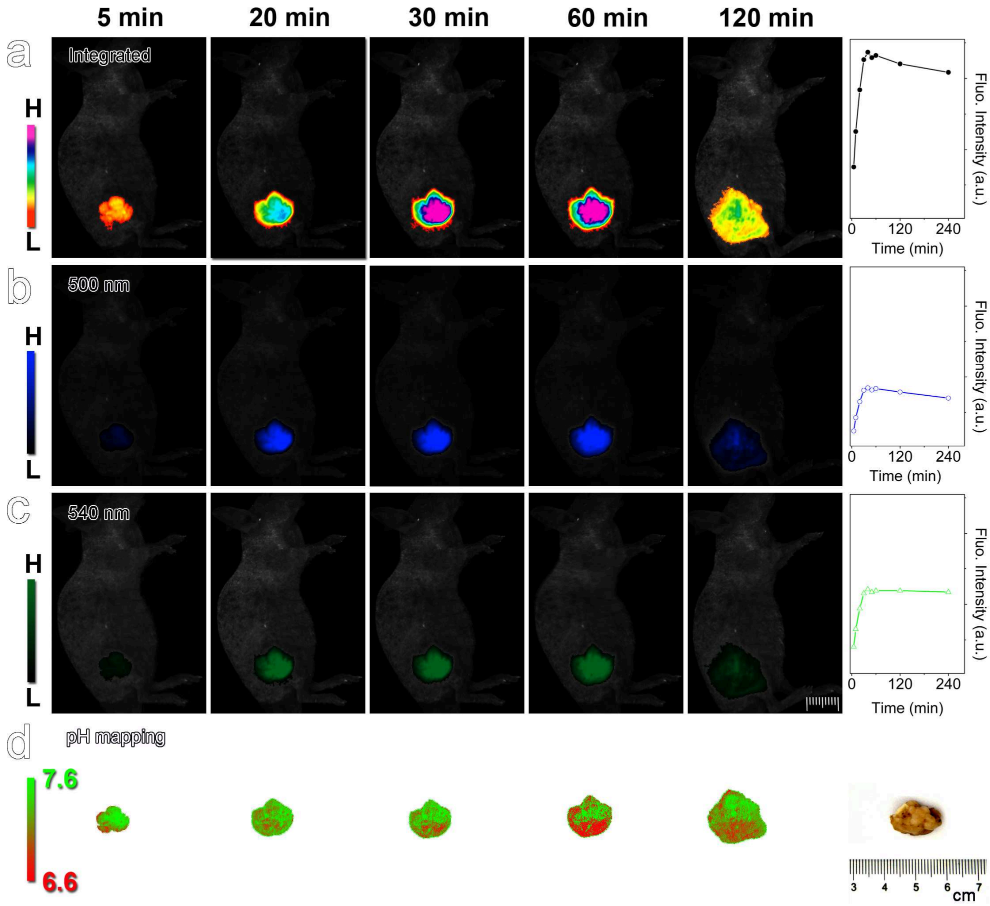


**Figure 3 | Fluorescence imaging of tumor *in vivo*.** Color-coded fluorescence images of tumor-bearing mice based on emission of 500 nm - 600 nm (a), 500 nm (b), and 540 nm (c), with temporal variations of integrated optical intensity lying aside. Pictures in row d are pH-mapping of the tumor region with an optical image of the harvested tumor placing at right hand side.

**Fluorescence imaging of tumor *in vivo*.** On the basis of aforementioned results, *in vivo* imaging of subcutaneous SGC7901 tumor xenografts was carried out after intra-tumor injection of the nanoprobe. As shown in panel a of Fig. 3, the fluorescence from the tumor site becomes detectable 5 min postinjection and then increases all the way in intensity to reach a plateau region between 30 and 60 min postinjection, after that it slightly decreases in intensity but expands in size. In the meantime, the fluorescence intensity of the central tumor area becomes a little lowered. The appearance and following enhancement of the fluorescence from tumor region can be attributed to the probe activation through MMP-9, while the latter expansion of the fluorescent area can be interpreted by outward diffusion of the released chromophores that are much smaller than the initial nanoprobe. In 30 min time window in between the size and shape of the fluorescent area remain nearly unchanged. This can be attributed to the antibody that helps to hold the attached chromophore in the extracellular matrix, which is beneficial for extracting the extracellular pH information within tumor.

It should be mentioned that due to the limitation of our imaging facility, fluorescence at 500 nm and 540 nm instead of 480 nm and 510 nm were recorded for detecting the pH of tumor matrix though with reduced sensitivity. In general, the fluorescence recorded at 500 nm and 540 nm, respectively, behave rather in consistence with the integrated fluorescence as quantitatively shown panels a-c of Fig. 3. According to the results shown in Fig. 1d, the fluorescence intensity ratio of $I_{500}/I_{540}$ is generally above 1 around neutral pH, but it is inversed in the animal experiments due to the heavier absorption of shorter wavelength light by tissue[31]. Though accurately extracting the pH information solely based the two-dimensional (2D) optical imaging results remains difficult owing to the three-dimensional nature and inhomogeneous structure of a given tumor, the absorption and scattering of excitation and emission by both tumor tissue and the overlying skin, etc, semi-quantitative analysis was carried out by taking the absorption of skin into consideration. More detailed calibration processes on the optical signals are provided in SI.

The corrected $I_{500}/I_{540}$ ratio together with its pH dependency then allow pH-mapping of the tumor region. In brief, the pH falls in the range of 6.6-7.5 with an average value being around 6.8 for the entire tumor. The detailed results given in panel d of Fig. 3 further reveal that during the early stage of postinjection, the pH imaging contrast remains low but gradually enhanced against time. At around 60 min postinjection, the pH inhomogeneity of the entire tumor is maximized. It is deserved to mention that at this imaging time point, the size of 2D fluorescent image remains rather comparable with that for tumor extracted right after the imaging experiment (right corner of panel d). Thereafter, the pH imaging contrast is gradually reduced. In fact, the integrated fluorescence intensity only decreases by 5.1% from 1 h to 2 h postinjection, but the size of fluorescent area is obviously enlarged. Therefore, the following reduced pH contrast is reasonably attributed to the outward diffusion of the chromophores into healthy tissue whose pH is typically around 7.4. Assuming that the diffusion takes place isotropically, the chromophores get closer to skin also contribute to the reduced pH imaging contrast upon prolonged observation.

In summary, a protease-activating fluorescent probe is proposed and constructed based on FRET between ratiometric fluorescent dye and biocompatible $Fe_3O_4$ nanocrystals covalently coupled through a MMP-9 specific peptide substrate linker. *In vitro* cell studies prove that the resulting nanoprobe can effectively be activated by MMP-9 secreted by gastric cancer cell line SGC7901 through the detachment of the MMP-9 specific peptide linker. In addition, the detached chromophores can well tag the tumor cells *in vitro* through covalently coupled anti-tumor antibody. The *in vivo* imaging experiments in combination of semi-quantitative analysis further suggest that the current probe can be used for realizing sensitive pH-mapping of tumor microenvironment. Although extracting accurate tumor pH information by optical imaging remains in the lack of satisfying inhomogeneous model, the current study paves an effective way to achieve novel probes suitable for noninvasive analysis of tumor-associated microenvironment.

## References

[1] M.J. Farquharson, A. Al-Ebraheem, G. Falkenberg, R. Leek, A.L. Harris, D.A. Bradley, The distribution of trace elements Ca, Fe, Cu and Zn and the determination of copper oxidation state in breast tumour tissue using $\mu$SRXRF and $\mu$XANES, Phys. Med. Biol. 53 (2008) 3023-3037.

[2] A.F. Chambers, L.M. Matrisian, Changing view of the role of matrix metalloprotinases in metastasis, J. Natl. Cancer. Inst. 89 (1997) 1260-1270.

[3] B.A. Webb, M. Chimenti, M.P. Jacobson, D.L. Barber, Dysregulated pH: a perfect storm for cancer progression, Nat. Rev. Cancer 11 (2011) 671-677.

[4] M.E. Stearns, M. Wang, Type IV collagenase (M(r) 72,000) expression in human prostate: benign and malignant tissue, Cancer. Res. 53 (1993) 878-883.

[5] B. Davies, J. Waxman, H. Wasan, P. Abel, G. Williams, T. Krausz, D. Neal, D. Thomas, A. Hanby, F. Balkwill, Levels of matrix metalloproteases in bladder cancer correlate with tumor grade and invasion, *Cancer*. *Res*. 53 (1993) 5365-5369.

[6] M.A. Moses, D. Wiederschain, K.R. Loughlin, D. Zurakowski, C.C. Lamb, M.R. Freeman, Increased incidence of matrix metalloproteinases in urine of cancer patients, Cancer. Res. 58 (1998) 1395-1399.

[7] M. Egeblad, Z. Werb, New functions for the matrix metalloproteinases in cancer progression, Nat. Rev. Cancer 2 (2002) 161-174.

[8] R.A. Gatenby, E.T. Gawlinski, A.F. Gmitro, B. Kaylor, R.J. Gillies, Acid-mediated tumor invasion: a multidisciplinary study, Cancer. Res. 66 (2006) 5216-5223.

[9] C. Stock, A. Schwab, Protons make tumor cells move like clockwork, Pflugers Arch. 458 (2009) 981-992.

[10] R. Weissleder, V. Ntziachristos, Shedding light onto live molecular targets, Nat. Med. 9 (2003) 123-128.

[11] R. Weissleder, C.H. Tung, U. Mahmood, A. Bogdanov, In vivo imaging of tumors with protease-activated near-infrared fluorescent probes, Nat. Biotechnol. 17 (1999) 375-378.

[12] C. Bremer, C.H. Tung, R. Weissleder, In vivo molecular target assessment of matrix metalloproteinase inhibition, Nat. Med. 7 (2001) 743-748.

[13] J. O. McIntyre, B. Fingleton, K.S. Wells, D.W. Piston, C.C. Lynch, S. Gantam, L.M. Matrisian, Development of a novel fluorogenic proteolytic beacon for in vivo detection and imaging of tumour-associated matrix metalloproteinase-7 activity, Biochem. J. 377 (2004) 617-628.

[14] Y. Zhang, M.K. So, J.H. Rao, Protease-modulated cellular uptake of quantum dots, Nano Lett. 6 (2006) 1988-1992.

[15] S. Lee, E.J. Cha, K. Park, S.Y. Lee, J.K. Hong, I.C. Sun, S.Y. Kim, K. Choi, I.C. Kwon, K. Kim, C.H. Ahn, A Near-infrared-fluorescence-quenched gold-nanoparticle imaging probe for in vivo drug screening and protease activity determination, Angew. Chem. Int. Ed. 47 (2008) 2804-2807.

[16] S. Nigam, K.C. Barick, D. Bahadur, Development of citrate-stabilized $Fe_3O_4$ nanoparticles: conjugation and release of doxorubicin for therapeutic applications, J. Magn. Magn. Mater. 323 (2011) 237-243.

[17] C. J. Yu, S. M. Wu, W. L. Tseng, Magnetite nanoparticle-induced fluorescence quenching of adenosine triphosphate-BODIPY conjugates: application to adenosine triphosphate and pyrophosphate sensing, Anal. Chem. 85 (2013) 8559-8565.

[18] J.H. Lee, Y.M. Huh, Y. Jun, J. Seo, J. Jang, H.T. Song, S. Kim, E.J. Cho, H.G. Yoon, J.S. Suh, J. Cheon, Artificially Engineered Magnetic Nanoparticles for Ultra-sensitive Molecular Imaging, Nat. Med. 13 (2007) 95-99.

[19] J. Zhou, C. L. Fang, T.J. Chang, D.H. Shangguan, A pH Sensitive Ratiometric Fluorophore and Its Application for Monitoring the Intracellular and Extracellular pHs Simultaneously, J. Mater. Chem. B 1 (2013) 661-667.